Water-Soluble Polymers. 80. Rheological and Photophysical Studies of pH-Responsive Terpolymers Containing Hydrophobic Twin-Tailed Acrylamide Monomers

Geoffrey L. Smith and Charles L. McCormick*

Department of Polymer Science, The University of Southern Mississippi, Southern Station, Box 10076, Hattiesburg, Mississippi 39406-0076

Received September 7, 2000; Revised Manuscript Received May 18, 2001

ABSTRACT: To examine the effects of microblock hydrophobicity on interpolymer association behavior, a series of terpolymers composed of acrylic acid, methacrylamide, and a $DiC_{12}AM$, $DiC_{14}AM$, or $DiC_{16}AM$ twin-tailed hydrophobic monomer have been synthesized using micellar polymerization methods. The terpolymer incorporating the $DiC_{12}AM$ hydrophobe possesses the highest initial viscosity and lowest critical yield stress in aqueous solution, while the terpolymer incorporating the $DiC_{14}AM$ hydrophobic monomer showed a slightly lower initial viscosity and critical yield stress. The pH response of these terpolymers was examined via rheology and fluorescence energy transfer (NRET) measurements. Dynamic frequency sweeps measured as a function of solution pH reveal viscoelastic behavior consistent with a simple Maxwell model. It is proposed that the number density of network junctions and the residency of hydrophobes in the junctions increase with pH. NRET measurements performed on mixed, separately labeled $DiC_{12}AM$ terpolymers indicate the onset of association (C^*) at ∼0.04 g/dL. Both NRET and steady shear viscosity studies indicate reorganization of the terpolymer network at pH values between 6.5 and 9.5, allowing for greater interaction of fluorescence labels and hydrophobes on separate chains.

Introduction

Incorporation of hydrophobic comonomers along an otherwise water-soluble polymer backbone utilizing micellar polymerization affords amphiphilic polymers having "microblocky" architecture.[1−4] These polymers when solubilized in aqueous media form interpolymer (open) associations which are responsible for increased solution viscosity at concentrations above C^*. The shear-reversible behavior of such networks is characteristic of associative thickening (AT) polymers.[5,6] At concentrations below C^*, these polymers often exhibit intrapolymer (closed) association. Transition from closed to open association in ATs can be "triggered" by incorporating pH-responsive functionality into the polymer backbone.

Some of the first microblocky ATs to be synthesized were reported by Evani[7] and Turner et al.[8] Around the same time McCormick and Johnson[9,10] synthesized similar hydrophobically modified polyacrylamides. These ATs contained small amounts of hydrophobic *n*-alkylacrylamide comonomers, including *n*-octyl (C_8AM), *n*-decyl ($C_{10}AM$), and *n*-dodecyl ($C_{12}AM$) acrylamides incorporated into the monomer feed at levels below 0.75 mol %. Copolymerization of small amounts of these hydrophobic comonomers led to dramatic increases in the viscosity of aqueous solutions as compared to homopolyacrylamide. Later, Middleton and McCormick[11,12] synthesized terpolymers of acrylamide (AM) with 0.5 mol % of either *N*-(*n*-decyl)acrylamide ($C_{10}AM$) or *N*-(4-butyl)phenylacrylamide (BPAM) as the hydrophobic comonomer and sodium acrylate (NaA), sodium 3-acrylamido-3-methylbutanoate (NaAMB), or sodium 2-acrylamido-2-methylpropanesulfonate (NaAMPS) as the anionic comonomers. All terpolymers exhibited good associative thickening properties in deionized water, and the carboxylate-based terpolymers exhibited a highly pronounced associative response relative to NaAMPS-containing polymers in high ionic strength environments. Terpolymers containing NaA associated more strongly than NaAMB-containing polymers; the effects of functional group distance from the backbone and conformational mobility appear to account for this behavior.

Similarly, Branham and McCormick[13] examined the effect of pH and polymer composition on the associative properties terpolymers of AM, AA, and *N*-(4-hexyl)-phenylacrylamide (HPAM). In these experiments, the hydrophobe content, sequence distribution, and molecular size were held constant, but the AA content of the terpolymers was varied. The solution behavior was characterized using rheometry and fluorescence probe techniques. Terpolymers containing 9 and 21 mol % AA exhibited extensive intermolecular associations at low pH (4.0−5.0) as well as in the presence of NaCl at higher pH. A terpolymer containing 37 mol % AA showed no rheological evidence of intermolecular associations throughout the pH range examined. Fluorescence experiments using pyrene probes confirmed that this polymer formed intramolecular hydrophobic microdomains. This study demonstrated that the association behavior of ATs could be controlled by tailoring the composition to respond in a specific manner to environmental stimuli including the solution pH and electrolyte concentration.[13]

Recently, Candau et al.[14] have studied the associative behavior of microblocky polymers composed of acrylamide and *N*,*N*-dihexylacrylamide. They demonstrated that N,N-disubstituted alkylacrylamido monomers enhance the associative behavior of hydrophobically modified polyacrylamides. Copolymers of AM and *N*,*N*-dihexylacrylamide displayed solution viscosities much higher than those of acrylamide and "single-tailed" hydrophobic comonomers. The stronger intermolecular association behavior was attributed to the greater hydrophobicity and increased microblocky character of the polymers.

10.1021/ma001554p CCC: $20.00
Published on Web 07/06/2001

Concurrent with the above research, our group has been examining the association efficiency of pH-responsive, microblocky ATs incorporating hydrophobic, twin-tailed monomers (from *N*,*N*-dihexylacrylamide up to *N*,*N*-didecylacrylamide).[23,24] These systems differ from those studied by Candau et al. since ionizable monomers are incorporated to promote solubility and stimuli responsiveness. We have recently reported our findings on the polymers incorporating *N*,*N*-dihexylacrylamide, *N*,*N*-dioctylacrylamide, and *N*,*N*-didecylacrylamide.[23,24] For these we found that lengthening the hydrophobe provided for enhanced network formation at lower concentrations and improved associative thickening.

On the basis of these findings, we now describe ATs prepared from monomers with extended twin alkyl chains (*N*,*N*-didodecylacrylamide, *N*,*N*-ditetradecylamide, and *N*,*N*-dioctadecylacrylamide) with the objective of determining the extent to which improvements in associative thickening can be realized prior to reaching the limits of solubility. Rheological and nonradiative energy transfer (NRET) fluorescence data are examined as a function of polymer concentration and solution pH for these new systems, and comparisons are made with lower alkyl twin-tailed analogues.

Experimental Section

Materials and Monomers. All chemicals were purchased from Fisher Chemical Co. or Aldrich Chemical Co. at the highest purity available. Purifications of VA-044 (water-soluble azo initiator) and methacrylamide (MAM) were accomplished by recrystallization from methanol and acetone, respectively. Acrylic acid (AA) was purified by vacuum distillation. All solvents and other materials were used as received unless otherwise indicated.

Syntheses of N,N-Didodecylamine, N,N-Ditetradecylamine, and N,N-Dihexadecylamine. Each of the disubstituted amines in the title compounds was synthesized by reacting 0.3 mol of the appropriate *N*-alkylamine with 0.3 mol of the corresponding alkyl bromide in 300 mL of acetonitrile in a 500 mL round-bottom flask equipped with an overhead stirrer and a condenser. The mixture was heated on a heating mantle, and the solution was refluxed for 6 h. Upon cooling, the resulting amine salt was found to solidify. The salt was filtered, dried, and extracted in methylene chloride using 6 M NaOH to deprotonate the salt. The extracted methylene chloride was then concentrated on a rotary evaporator, and the resulting diamine was dried in vacuo and weighed to give 71, 57, and 52% yield and mp (salt) 33−34, 34−36, and 33−37 °C, respectively. TLC analysis using a chloroform/acetone mixture indicated a single product.

Syntheses of N,N-Didodecylacrylamide ($DiC_{12}AM$), N,N-Ditetradecylacrylamide ($DiC_{14}AM$), and N,N-Dihexadecylacrylamide ($DiC_{16}AM$). Methylene chloride (100 mL), 0.100 mol of *N*,*N*-didodecylamine, *N*,*N*-ditetradecylamine, or *N*,*N*-dihexadecylamine, and 6 N sodium hydroxide (50 mL) were added into a 500 mL three-neck, round-bottomed flask. The mixture was placed in an ice bath and agitated vigorously using an overhead stirrer under a dry nitrogen atmosphere. When the temperature dropped below 10 °C, acryloyl chloride (0.104 mol) in methylene chloride (25 mL) was added slowly from an addition funnel such that the temperature was maintained below 10 °C. The mixture was stirred for an additional 2 h after complete addition of acryloyl chloride. The organic layer was then separated in a 500 mL separatory funnel, washed twice with water and once with concentrated NaCl solution, and dried over anhydrous magnesium sulfate. The solvent was removed on a rotary evaporator to yield a light yellow oil (yield 91%, 82%, and 87%, respectively). TLC analysis using a chloroform/acetone mixture confirmed product purity. DiC_{12}-AM: Anal. ^{1}H NMR ($CDCl_3$): δ 0.85−0.91 ($-CH_3$), 1.27 ($-CH_2-$), 1.56 ($-CH_2-CH_3$), 3.25−3.40 ($-N-CH_2-$), 5.62−5.68 (1H $=CH_aH_b$). 6.29−6.38 (1H $=CH-$), 6.48−6.62 (1H $=CH_aH_b$) ^{13}C NMR ($CDCl_3$): δ 17.1, 21.1, 25.5, 29.8, 32.3, 32.6, 34.9, 42.5 (CH_2, CH_3), 61.0 ($NH-CH_2$), 128.6 ($=CH_2$), 134.1 ($CH_2=$), 168.5 (C=O). 17.1, 21.1, 25.5, 29.8, 32.3, 32.6, 34.9, 42.5 (CH_2, CH_3), 61.0 ($NH-CH_2$), 128.6 ($=CH_2$), 134.1 ($CH_2=$), 168.5 (C=O). FT-IR (KBr): C−H stretch, 2926, 2855; N−C=O stretch 1654, C=C stretch 1615, C−H bend 1456, 1377, 977, CH_2 rock 723. $DiC_{14}AM$ and $DiC_{16}AM$ exhibited virtually identical peak positions, with proton NMR integration showing the additional methylene groups.

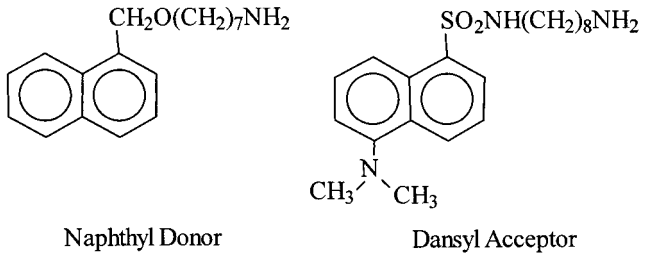

Figure 1. Fluorescence chromophores utilized for fluorescence energy transfer experiments.

Fluorescence Labels. Dansyl-2-aminocaprylic acid and succinic acid *N*-(1-naphthylmethyl) monoamide were chosen as model compounds. The former was purchased from Sigma and was recrystallized from methanol. The nonradiative energy transfer (NRET) donor used for labeling the copolymer backbone was 7-(1-naphthylmethoxy)heptylamine, synthesized using the methods of McCormick and Chang.[15] The NRET acceptor, 8-dansyloctylamine, was synthesized as described by Shea et al.[16] The structures of these chromophores are shown in Figure 1.

Micellar Polymerization. Co- and terpolymers were synthesized by micellar polymerization using sodium hexadecyl sulfate (SHdS) to solubilize the hydrophobic comonomer and VA-044 as the free-radical initiator. The total monomer concentration was held constant at 0.44 M and the [monomer]/[initiator] ratio at 2000. Also, the hydrophobic monomer content and the surfactant-to-hydrophobic monomer ratio (SMR) were held constant at 1 mol % and 28, respectively. The aggregation number and cmc used to calculate the required amount of SHdS were 74 and 0.54 mM, respectively.[25] The reactions were conducted for 3−6 h at 60 °C. The feed ratio of monomers (Figure 2) in all polymerizations was held at 49/50/1.

In a typical polymerization, deionized water (600 mL) was sparged with N_2 for 30 min. SHdS (23.5 g) was added with stirring under N_2 purge. $DiC_{12}AM$ (1.01 g) was then added with continued stirring for approximately 1 h or until the solution cleared. MAM (10.5 g) and AA (8.90 g) were then dissolved in the reaction mixture. The pH of the reaction feed was measured and adjusted to keep the AA moieties in their protonated form. VA-044 (0.039 g) was dissolved in 5 mL of deoxygenated, deionized water and injected into the polymerization vessel. The reaction was allowed to proceed under N_2 for 6 h, after which the terpolymer was precipitated into 1000 mL of methanol. The terpolymer was then washed with fresh methanol and dried overnight in a vacuum oven. Further purification was achieved by redissolving the terpolymer in water and dialyzing against deionized water for 5 days using Spectra Por No. 4 dialysis tubing with a molecular weight cutoff of 12 000−14 000. The purified polymer samples were then freeze-dried to a constant weight. Synthetic parameters for the other co- and terpolymers made in this study appear in Table 1.

Fluorescence Labeling. The MAM/AA/$DiC_{12}AM$ terpolymer was dissolved in a 70/20 dioxane/formamide mixed solvent system. The appropriate fluorescence label was added to the solution along with the typical 1,3-dicyclohexylcarbodiimide (DCC)/4-(dimethylamino)pyridine (DMAP) mixture, and the solution was heated to 60 °C and allowed to react overnight. The details of this reaction are given elsewhere.[17] The resulting solutions were then poured into Spectra Por No. 4 dialysis tubing and allowed to dialyze against deionized water for 15

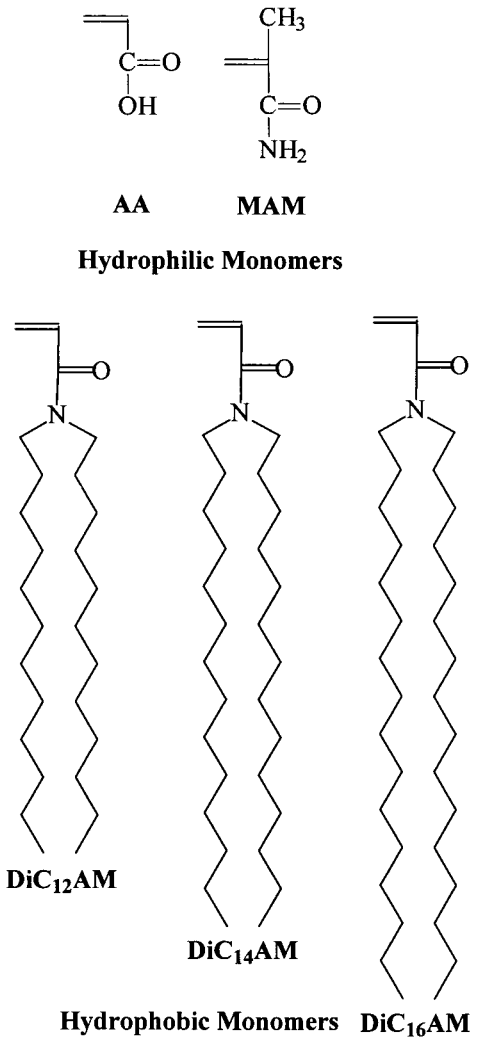

Figure 2. Hydrophilic monomers: acrylic acid (AA); methacrylamide (MAM) and hydrophobic monomers: *N*,*N*-didodecylacrylamide ($DiC_{12}AM$), *N*,*N*-ditetradecylacrylamide ($DiC_{14}AM$), and *N*,*N*-dihexadecylacrylamide ($DiC_{16}AM$).

Table 1. Synthetic Parameters Utilized for Micellar Polymerizations

sample	[Surf] (mol/L)	SMR	MAM (%)	AA (%)	hydrophobe (1 mol %)
MAM/AA/$DiC_{12}AM$	0.11	28	49.0	50.0	$DiC_{12}AM$
MAM/AA/$DiC_{14}AM$	0.11	28	49.0	50.0	$DiC_{14}AM$
MAM/AA/$DiC_{16}AM$	0.11	28	49.0	50.0	$DiC_{16}AM$

days. The purified, labeled polymer samples were then freeze-dried to a constant weight. Using UV and Beer's law to determine label incorporation, we found 0.42 mol % for the dansyl label and 0.57 mol % for the naphthyl label.

Analytical Methods. *Light Scattering Measurements.* Measurements of d*n*/d*c* were performed with a Chromatix KMX-16 laser differential refractometer ($\lambda = 632.8$ nm). MAM/AA terpolymer d*n*/d*c* values and apparent molecular weights were determined in 0.5 M NaCl. Dust was removed from samples via centrifugation in a Brinkmann Instruments (5415C) Eppendorf microcentrifuge at 16 000*g* until no visible scattering due to dust was observed (30 min−5 h). Classical light scattering was performed using a Brookhaven Instruments BI-200SM automatic goniometer attached to a Spectra Physics He−Ne laser operating at 632.8 nm. Using standard Zimm analysis, the apparent molecular weights and radii of gyration were obtained. All dilution solvents were also cleaned by filtration though 0.45 μm filters to remove dust. Multiple analyses were performed to ensure reproducibility.

Fluorescence Quantum Yield. Prior to quantum yield determination, the absorbance of the dansyl labels at 330 nm for a polymer concentration of 0.50 g/L was determined. Fluorescence quantum yield was then calculated using eq 1,

$$\Phi_x = \Phi_{st} \frac{A_{st}}{A_x} \frac{I_x}{I_{st}} \frac{{n_x}^2}{{n_{st}}^2} \tag{1}$$

in which Φ is the quantum yield, A is the absorbance at the excitation wavelength, I is the integral area of the corrected emission spectrum, and n is the refractive index at the excitation wavelength. The subscript x refers to the utilized chromophore, and the subscript st refers to the standard compound.

Nonradiative Energy Transfer. For NRET measurements, an Acton cutoff WG-305 optical filter was used at the excitation wavelength (282 nm) to prevent scattering of the excitation beam from the samples. The dansyl chromophores were excited at 330 nm to observe the dansyl emission spectra. Quantum yields (Φ) of the fluorescent labels were calculated by integrating the areas of the corrected emission spectra in reference to 2-aminopyridine in 0.10 N H_2SO_4 as the standard ($\Phi = 0.60$ at 282 nm excitation).[18] Quantum yields (Φ) of the dansyl groups excited at 330 nm were calculated by integrating the areas of corrected emission spectra in reference to quinine bisulfate in 1.0 N H_2SO_4 as the standard ($\Phi = 0.55$ at 330 nm excitation).[19] Beer's law corrections were applied for optical density changes at the excitation wavelength. Corrections were also made for refractive index differences.

The Förster distance, r_0, has been previously determined to be 23.45 Å for the naphthalene/dansyl donor/acceptor pair,[20] and the NRET quantum efficiency, χ, has been calculated using the method described by Guillet.[21] In this case, the modified Guillet method[22] is used for calculating NRET quantum efficiency, χ, due to the minor absorbance of the dansyl chromophore at the excitation wavelength of 282 nm. The modified Guillet equation is shown in eq 2

$$\frac{\chi}{1-\chi} = \frac{\Phi_D^0 (I_A - I_A^0)}{\Phi_A^0 I_D} \tag{2}$$

in which Φ_D^0 is the fluorescence emission quantum yield of the donor in the absence of acceptor-labeled polymer excited at 282 nm and Φ_A^0 is the fluorescence emission quantum yield of the acceptor on the acceptor-labeled polymer. I_A and I_D are the integrated emission intensities of donor and acceptor, respectively, in the presence of both donor- and acceptor-labeled polymer, and I_A^0 is the integrated emission intensity of the acceptor in the absence of donor-labeled polymer.

Steady-State and Dynamic Rheology. The rheological properties of the more viscous polymer solutions were measured with a Rheometrics Scientific SR-5000 controlled-stress rheometer. All measurements were performed at 25 °C using a cone and plate attachment with a 2° angled cone with a 25 mm diameter. Steady shear and dynamic measurements were conducted to obtain the steady shear viscosity and the dynamic viscoelastic properties of the studied polymer solutions. To negate any shear history effects, each sample was subjected to a 5 min preshear of 10 s^{-1} for 5 min, followed by a 5 min rest period prior to measurement. The oscillatory shear measurements were performed within the linear viscoelastic regime, where the storage (G') and loss (G'') moduli were found to be independent of the strain amplitude.

Results and Discussion

Monomer Selection, Synthesis, and Characterization. The monomers chosen for this study are shown in Figure 2. Acrylic acid and methacrylamide were utilized at a 50:49 ratio to allow sufficient hydrophilicity and pH responsiveness. The DiC_{12}, DiC_{14}, or DiC_{16} twin-tailed monomers were introduced into the feed at 1 mol

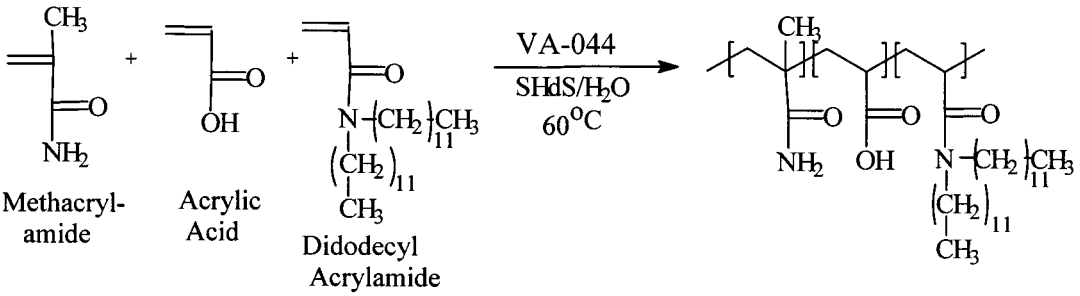

Figure 3. Micellar polymerization of methacrylamide, acrylic acid, and didodecylacrylamide.

Table 2. Molecular Weights and Radii of Gyration for Twin-Tailed Acrylamido Terpolymers

sample	hydrophobe	SMR	R_g (nm)	MW (g/mol) $\times 10^{-6}$
MAM/AA/DiC_{12}AM	DiC_{12}AM	28	42.2	0.982
MAM/AA/DiC_{14}AM	DiC_{14}AM	28	21.1	0.457
MAM/AA/DiC_{16}AM	DiC_{16}AM	28		insoluble

%, anticipating strong associative interactions based on previous studies.[23,24] Since these twin-tailed monomers were not commercially available, we first synthesized the N,N-disubstituted amines and subsequently their corresponding monomers as outlined in the Experimental Section.

Polymer Synthesis and Molecular Weight Determination. Initially, micellar polymerization of the DiC_{12}AM, DiC_{14}AM, or DiC_{16}AM twin-tailed monomers with AA and MAM was attempted using sodium dodecyl sulfate (SDS) as the surfactant. However, SDS, at the concentrations required to make an appropriately microblocky polymer, did not sufficiently solubilize the DiC_{14}AM and DiC_{16}AM monomers. As a result, sodium hexadecyl sulfate (SHdS) was chosen to maintain solubility during the polymerization. A typical polymerization scheme is shown in Figure 3; the compositions of the terpolymers synthesized are summarized in Table 1. During polymerization, all polymers remained soluble in the reaction solution. However, after subsequent surfactant removal and purification, the DiC_{16}AM terpolymer was not water-soluble, a characteristic of strong association often observed at high degrees of hydrophobic substitution. While addition of *N,N*-dimethylacetamide was found to assist in resolubilization in aqueous media, further study of this polymer will not be reported here. Classical light scattering with the standard Zimm analysis was utilized to determine weight-average molecular weights (M_w) and mean radii of gyration (R_g). The results for those terpolymers which were soluble in 0.5 N NaCl at pH 8 are provided in Table 2.

Rheological Properties. *Effects of Shear Stress and Hydrophobe Length on Solution Viscosity.* Steady shear viscosities (η) as a function of shear stress are shown in Figure 4 for the DiC_{12}AM and the DiC_{14}Am terpolymers at a concentration of 1.0 g/dL and a pH value of 8. Also, shown is the steady shear viscosity for the previously reported DiC_{10}AM terpolymer.[24] At these concentrations the polymers are well above their respective overlap concentrations (C^*) and exist in highly networked states. As a result, all three polymer exhibit high critical yield stresses for network deformation. The shapes of all three curves are quite similar, although response values differ by decades. At low shear stresses, a small shear-thickening regime is observed. A short plateau region where the viscosity remains relatively constant with increasing shear stress follows at intermediate shear stresses. At higher shear stresses, the samples become shear thinning and exhibit decreases in viscosity characterized by two different slopes. This behavior is characteristic of two distinct changes in the structure of the polymer network occurring at different critical shear stresses, the first being more dramatic than the second. Jenkins et al.[6] have observed similar shear stress profiles for hydrophobically modified alkali-swellable emulsion (HASE) ATs and have attributed the initial more abrupt change to the catastrophic disruption of the polymer network. At the onset of shear thinning, hydrophobic units are in equilibrium between associated and dissociated states. With increasing shear stress in this regime, this equilibrium becomes increasingly shifted to the dissociated state and a dramatic decrease in viscosity is observed. An explanation for the second, structural change is less clear. Under these conditions of shear, the forces placed on the polymer network are such that the interpolymer association equilibrium is shifted almost completely toward the dissociated state.

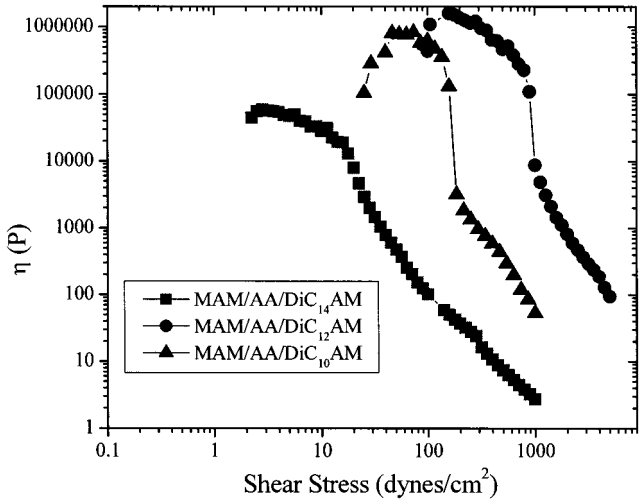

Figure 4. Steady shear viscosities (η) as a function of shear stress for DiC_{10}AM, DiC_{12}AM, and the DiC_{14}Am terpolymers at a concentration of 1.0 g/dL at a pH value of 8.0.

In comparing the steady shear viscosity curves for each of the polymers, the effect of twin-tail hydrophobicity on aqueous solution viscosity is readily apparent (Figure 4). The terpolymer incorporating the DiC_{12}AM hydrophobic monomer shows the most pronounced initial viscosity and highest critical stress required to cause network deformation, followed by the terpolymers incorporating the DiC_{10}AM and DiC_{14}AM hydrophobic monomers, respectively. The less desirable behavior of the DiC_{14}AM terpolymer is most likely the result of lower molecular weight and insufficient solubility to promote effective associative thickening. Of the three

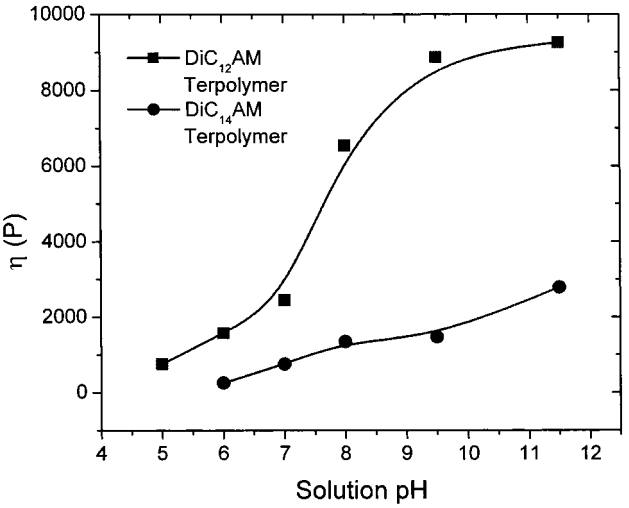

Figure 5. Steady shear plateau viscosity vs pH for $DiC_{12}AM$ and $DiC_{14}Am$ terpolymers at a concentration of 0.5 g/dL.

terpolymers, polymerized under specific conditions outlined in the Experimental Section, an apparent maximum in AT behavior is reached when the alkyl chain length has a carbon number of 12.

Effect of pH on Viscosity Behavior. Incorporation of AA into the terpolymer backbone allows for water solubility and provides pH responsiveness. To investigate the effects of pH on chain expansion of the networked microblocky ATs, the viscosity as a function of pH for both the $DiC_{12}AM$ and $DiC_{14}Am$ terpolymers at a concentration of 0.5 g/dL was examined (Figure 5).

For the $DiC_{12}AM$ terpolymer, a slight increase in viscosity is observed between pH values of 5 and 7. At the lowest pH value, the polymer is only marginally soluble in aqueous solution and likely exists in a collapsed state with most hydrophobes participating in intrapolymer vs interpolymer associates. As the pH is increased over this range (5−7), the polymer becomes partially ionized, and limited chain (backbone) extension occurs. At pH values between 7 and 11, a larger change in viscosity for the $DiC_{12}AM$ terpolymer is observed. Ionization of the carboxy functional groups into a conformationally extended, energetically favorable state occurs. At these pH values the degrees of ionization are sufficient to overcome hydrophobic forces and disrupt intrapolymer aggregates, resulting in reordered, extended structures with more efficient network formation. The less pronounced behavior of the $DiC_{14}AM$ terpolymer is again likely due to its lower molecular weight and more hydrophobic nature. Solvation and conformational rearrangements with increasing pH are not as favorable. The pH-responsive behavior of both terpolymers is illustrated in Figure 6.

pH-Responsive Viscoelastic Behavior of Microblocky Twin-Tailed Terpolymer Networks. Dynamic rheology measurements allow the selective probing of chain conformations and/or network states.[26−28] Experimental data can be fit to an idealized Maxwell viscoelastic model to assess the dynamic behavior of these polymers. Candau et al.[14] have suggested the model to be appropriate for microblocky ATs at intermediate concentrations. In this study, we have examined the pH-dependent behavior of the $DiC_{12}Am$ and the $DiC_{14}Am$ terpolymers at a fixed polymer concentration in order to observe the role that pH plays in their dynamics in solution. The resulting data were fit to a simple Maxwell

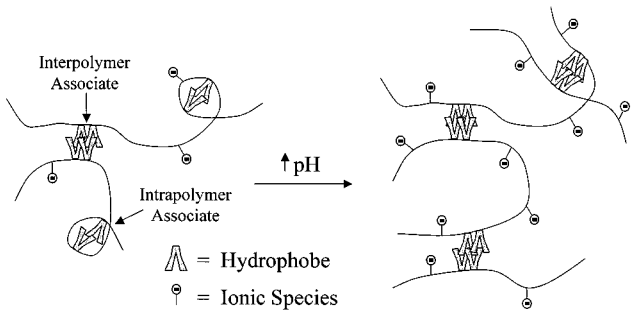

Figure 6. Model illustrating the effect of solution pH on terpolymer association behavior.

model which characterizes polymer systems in terms of an elastic (G') and viscous (G'') moduli described by eqs 3 and 4, respectively

$$G'(\omega) = G_0\omega^2\lambda^2/(1 + \omega^2\lambda^2) \quad (3)$$

$$G''(\omega) = G_0\omega\lambda/(1 + \omega^2\lambda^2) \quad (4)$$

where G_0 is the plateau modulus and λ is the terminal relaxation time at all frequency (ω) values. Thus, $G'(\omega)$ and $G''(\omega)$ were determined for the $DiC_{12}Am$ and the $DiC_{14}Am$ terpolymers as functions of ω at selected pH values and fixed polymer concentrations of 0.5 g/dL.

Figure 7 represents typical dynamic frequency sweep plots and their fits obtained for the $DiC_{12}Am$ and the $DiC_{14}Am$ terpolymers at pH 7. Both plots in Figure 7 indicate that at low frequencies the viscous features of each polymer predominate ($G'' > G'$), while at higher frequencies the G' curve overtakes the G'' curve, indicating the predominance of the elastic response. The increasing viscoelastic behavior of these polymers with frequency is characteristic of entangled polymer networks.[26,27]

Experimental $G'(\omega)$ and $G''(\omega)$ data for each sample were found to exhibit a relatively good fit to the theoretical model based on a single-element Maxwell model (represented by the solid lines in Figure 7). From the fits using eqs 3 and 4, G_0 and λ at each pH value were determined and are plotted in Figure 8 for the terpolymers studied. Both G_0 and λ exhibit increases with pH for the $DiC_{12}AM$ terpolymer, with large increases in both values being observed between pH 7 and 9.5. The G_0 and λ curves for the $DiC_{14}AM$ terpolymer are similar but exhibit less dramatic changes with increasing pH values. Interpretation of these data can be attempted using simple rubbery elasticity theory extended to transient networks by Green and Tobolsky.[29] According to this theory, the magnitude of G_0 is proportional to the number density of mechanically active chains in the network. As mentioned above, network junctions behave transiently with the junctions being in an equilibrium state of disruption and reformation. The lifetime of a junction depends on the residence time of a hydrophobe occupying a space in the junction aggregate. The faster that hydrophobes exit the junction, the shorter this time will be. According to transient network theory, the lifetime of these junctions is directly related to the terminal relaxation time.[29] Thus, the results in Figure 8 indicate that, with increasing solution pH, the number density of network junctions increases as does the lifetime of a twin-tailed hydrophobe in a junction. This observation is consistent with a reorganization of network junctions caused by an

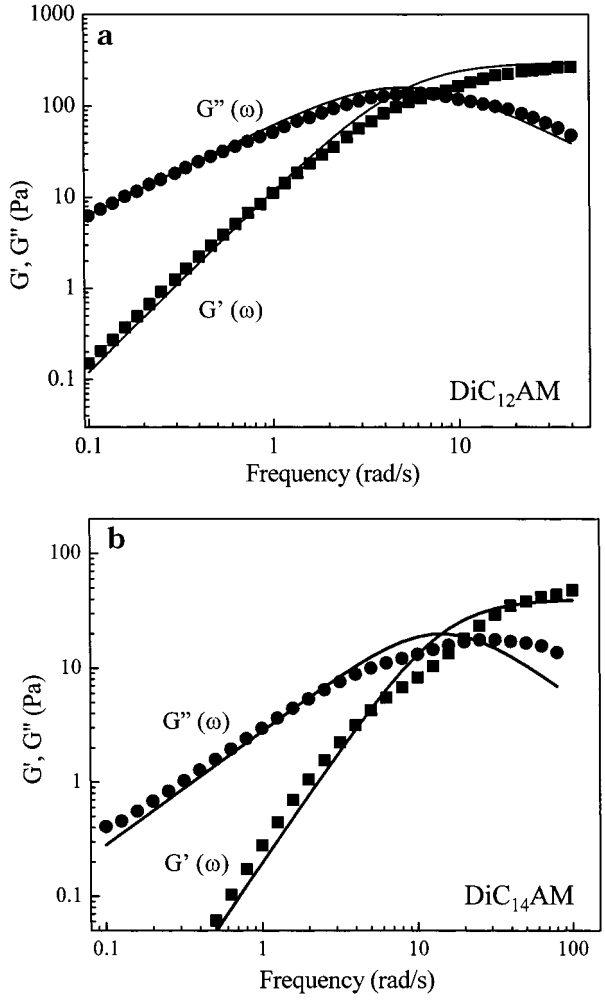

Figure 7. Dynamic frequency sweep study and subsequent fitting for the $DiC_{12}AM$ and $DiC_{14}AM$ terpolymers (0.5 g/dL) at pH 7 with $\tau = 300$ and 20 dyn/cm^2, respectively.

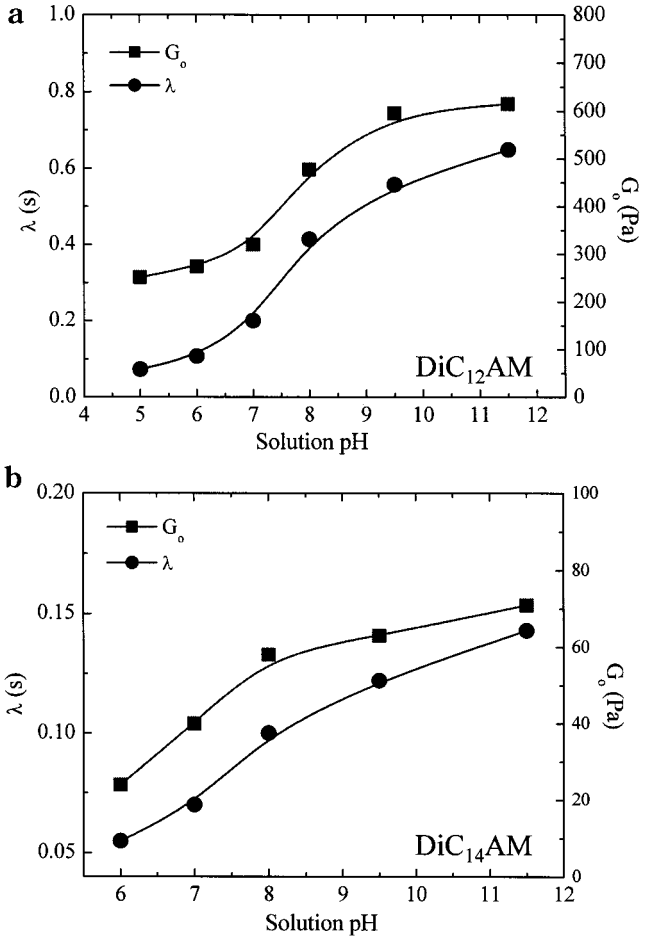

Figure 8. G_0 and λ as a function of solution pH for the DiC_{12}-AM and $DiC_{14}AM$ terpolymers (0.5 g/dL).

increase in the solution pH. At lower pH values the network aggregates may be largely intrapolymer in nature. However, as the pH increases and chain expansion occurs, the hydrophobes are able to reorganize and form more effective interpolymer network junctions.

Fluorescence Energy Transfer Measurements. To gain a more complete understanding of the solution behavior, the twin-tailed, $DiC_{12}Am$ terpolymer was labeled with naphthyl and dansyl chromophores. The effect of polymer concentration and solution pH on nonradiative energy transfer (NRET) behavior was then examined by performing measurements on mixed polymer solutions following a procedure previously reported by Hu and McCormick.[30] The Förster distance for this energy transfer pair has previously been documented as 23.45 Å.[20] This distance corresponds to that in which the energy transfer efficiency between chromophore pairs is 50%. This method provides a very sensitive means of indicating hydrophobic association and network formation at the molecular level.

Effect of Polymer Concentration on Energy Transfer. Figure 9 illustrates the emission intensity vs wavelength behavior for the mixed, individually labeled chains containing the dansyl and naphthyl chromophores for five different polymer concentrations when the naphthyl donor was excited at 282 nm. As the total polymer concentration is increased, more naphthyl and dansyl donor and acceptor pairs come within the Förster

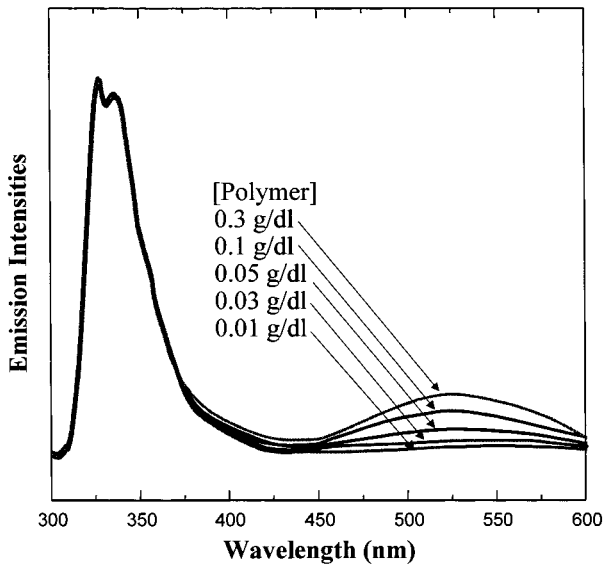

Figure 9. Normalized emission spectra for MAM/AA/DiC_{12}-AM polymers excited at 282 nm at pH 8.0 and 25 °C.

distance and energy transfer occurs as evidenced by an emission increase in the dansyl region between 450 and 580 nm. At the lowest polymer concentrations (0.01 and 0.03 g/dL) little emission in this region is observed. Significant energy transfer begins at a concentration of ~0.05 g/dL. While this energy transfer behavior is not readily apparent by examination of the emission spectra, a clearer indication of the amount of energy

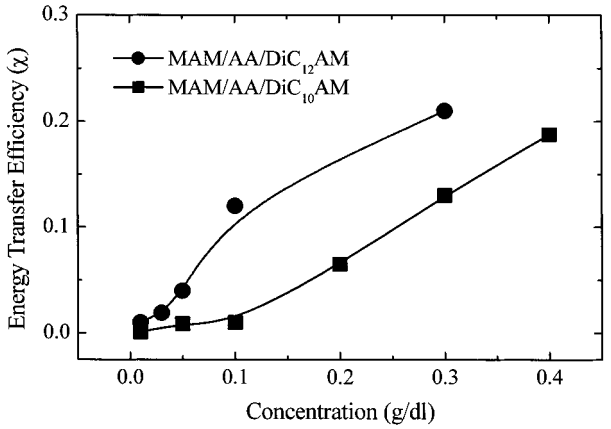

Figure 10. Energy transfer efficiency plot for labeled MAM/AA/DiC_{10}AM and MAM/AA/DiC_{12}AM terpolymers with naphthalene and dansyl labels mixed in equimolar amounts at pH 8.0 and 25 °C.

transferred may be obtained by plotting the NRET quantum efficiency vs polymer concentration for the mixed labeled DiC_{12}AM terpolymer at pH 8. Using the Guillet equation, the NRET quantum efficiency can by calculated at each concentration. This allows for the determination of the microscopic overlap concentration at which labels begin to interact. These data for the DiC_{12}AM terpolymer are shown in Figure 10 along with data from the DiC_{10}AM terpolymer discussed previously.[24]

A large increase in NRET quantum efficiency occurs at ~0.04 g/dL for the DiC_{12}AM terpolymer. Change in the slope at this concentration is indicative of initial chain overlap and the onset of network formation. At concentrations below 0.04 g/dL, most polymer chains likely exist as unimers in solution. The small amount of energy transfer occurring at these concentrations results from the occasional diffusional encounter of chains. Above 0.04 g/dL, interpolymer association occurs and significant energy transfer is observed. A comparison of the DiC_{12}AM terpolymer and the DiC_{10}AM terpolymer previously reported[24] reveals that the onset of intermolecular association occurs at a lower concentration in the former. This behavior is consistent with a model provided for the concentration-dependent association behavior of the DiC_{10}AM terpolymer discussed in a previous publication.[24]

Effect of Solution pH on Energy Transfer. To verify the effects of solution pH on terpolymer network expansion and dynamics as determined from rheology measurements, NRET experiments were performed on mixed, individually labeled DiC_{12}AM terpolymers at a fixed concentration of 0.1 g/dL as a function of pH. After making corrections for the direct excitation of the dansyl label at 282 nm, the Guillet equation was utilized to calculate the NRET quantum efficiency at six pH values between 5 and 11.5. These data are provided in Figure 11.

Close examination reveals that the NRET behavior follows viscosity behavior. A small increase in viscosity is observed between pH values of 5 and 6.5 with an inflection point at approximately 6.5. Because of the high hydrophobicity of the DiC_{12}Am species, the number of intrapolymer associations at these pH values is most likely high. With increasing pH, the polymer becomes increasingly more soluble; however, ionic repulsions at low pH values are not sufficient to cause significant network reorganization. At pH values between 6.5 and

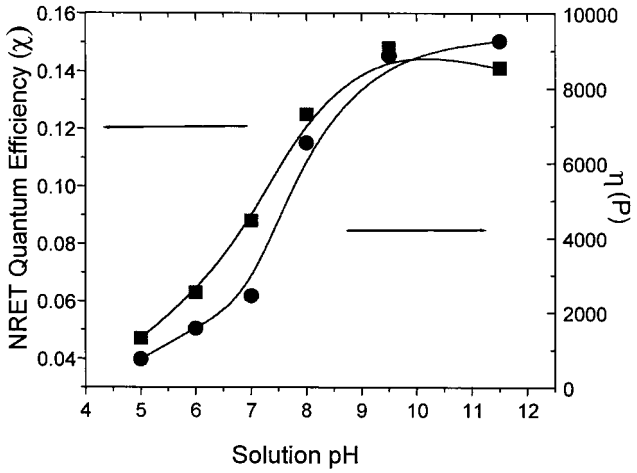

Figure 11. Energy transfer efficiency and steady shear viscosity vs pH for labeled DiC_{12}AM terpolymer at fixed concentrations of 0.1 and 0.5 g/dL, respectively.

9.5, a large change in NRET is observed. At these higher pH values, ionic repulsion overcomes hydrophobic association at the network junction, and the polymers rearrange to form more favorable intermolecular networks. At pH 11.5 a slight decrease in NRET is observed. This is most likely a result of network collapse caused by shielding at high ionic strength. This NRET behavior is similar to that previously observed for a similar DiC_{10}Am terpolymer[24] and is consistent with recent reports by Iliopoulos[31,32] showing NMR evidence for both intra- and interpolymer aggregation of hydrophobically modified poly(sodium acrylate) across the entire concentration regime.

Conclusions

Previous studies performed on twin-tailed associative terpolymers having DiC_6, DiC_8, or DiC_{10} hydrophobic groups indicated that the greater the hydrophobe chain length, the more pronounced the viscosity enhancement.[23,24] This was attributed to formation of stronger network junctions at lower concentrations by the more hydrophobic microblocks. Solubility problems, however, led us to incorporate comonomers with hydrophilicity and pH responsiveness. Thus, a series of terpolymers consisting of 49 mol % of MAM, 50 mol % of AA, and 1 mol % of DiC_{12}AM, DiC_{14}AM, or DiC_{16}AM twin-tailed hydrophobic monomer were synthesized to investigate this behavior. The solubility limit was reached with the polymer containing the DiC_{16}AM hydrophobe, even at low concentrations and high pH values. The terpolymer incorporating the DiC_{12}AM hydrophobic monomer exhibited the most pronounced initial viscosity and highest yield stress, followed by the terpolymer incorporating the DiC_{14}AM hydrophobic monomer. The lower viscosity of the latter is thought to be due to higher hydrophobicity and thus closer proximity to the solubility limit.

The effects of solution pH on the expansion and dynamics of the polymer networks formed by these systems were also examined using rheology and fluorescence NRET measurements. The steady shear viscosity for both the DiC_{12}AM and DiC_{14}AM terpolymers increased with increasing pH, with a change in slope occurring at pH values around 7 and 8.5, respectively. These inflections represent critical pH values required to overcome hydrophobic association and to cause network reorganization into more expanded interpolymer associates. Dynamic frequency sweeps performed

on these systems as a function of solution pH revealed viscoelastic behavior consistent with a simple Maxwell model. It is proposed that the number density of network junctions and the residency of hydrophobes in the junctions increase with pH, a result of ionic repulsion and extension along the chain due to molecular level conformational changes. Fluorescence energy transfer measurements were also performed with labeled $DiC_{12}AM$ terpolymer and indicated the onset of association (C^*) at ~0.04 g/dL. Consistent with previous work, the onset of intermolecular association occurs at lower concentrations for terpolymers with more hydrophobic monomers. Finally, both NRET and viscosity studies indicate reorganization at pH values between 6.5 and 9.5 into a more effective interpolymer network as demonstrated by greater interaction of the fluorescence labels.

Acknowledgment. Financial support for this research from ICI, the Department of Energy, and the Office of Naval Research is gratefully acknowledged.

References and Notes

(1) Peer, W. In *Polymers in Aqueous Media*; Glass, J. E., Ed.; Advances in Chemistry Series No. 223; American Chemical Society: Washington, DC, 1989; p 381.
(2) Ezzell, S. A.; McCormick, C. L. In *Water Soluble Polymers. Synthesis, Solution Properties, and Applications*; Shalaby, S., McCormick, C. L., Butler, G. B., Eds.; ACS Symposium Series No. 467; American Chemical Society: Washington, DC, 1991; pp 130−150.
(3) Ezzell, S. A.; McCormick, C. L. *Macromolecules* **1992**, *25*, 1881.
(4) Ezzell, S. A.; Hoyle, C. E.; Creed, D.; McCormick, C. L. *Macromolecules* **1992**, *25*, 1887.
(5) Tam, K. C.; Jenkins, R. D.; Winnik, M. A.; Bassett, D. R. *Macromolecules* **1998**, *31*, 4149.
(6) Tirtaatmadja, V.; Tam, K. C.; Jenkins, R. D.; Bassett, D. R. *Colloid Polym. Sci.* **1999**, *277*, 276.
(7) Evani, S. U.S. Patent 4,432,881, 1984.
(8) Turner, S. R.; Siano, D. B.; Bock, J. U.S. Patent 4,528,348, 1985.
(9) McCormick, C. L.; Johnson, C. B. *PMSE Prepr.* **1986**, *55*, 366.
(10) McCormick, C. L.; Nonaka, T.; Johnson, C. B. *Polymer* **1988**, *29*, 731.
(11) McCormick, C. L.; Middelton, J. C.; Grady, C. E. *Polymer* **1992**, *33*, 4184.
(12) McCormick, C. L.; Middelton, J. C.; Cummins, D. F. *Macromolecules* **1992**, *25*, 1201.
(13) Branham, K. D.; Snowden, S. L.; McCormick, C. L. *Macromolecules* **1996**, *29*, 254.
(14) Regalado, E. J.; Selb, J.; Candau, F. *Macromolecules* **1999**, *32*, 8580.
(15) McCormick, C. L.; Chang, Y. *Macromolecules* **1994**, *27*, 2151.
(16) Shea, K. J.; Stoddard, G. J.; Shavelle, D. M.; Wakui, F.; Choate, R. M. *Macromolecules* **1990**, *23*, 4497.
(17) Boudreaux, C. J.; Bunyard, W. C.; McCormick, C. L. *J. Controlled Release* **1996**, *40*, 223.
(18) Rusakowicz, R.; Testa, A. C. *J. Phys. Chem.* **1968**, *72*, 2680.
(19) Eastmen, J. W. *Photochem. Photobiol.* **1967**, *6*, 55.
(20) Lakowicz, J. R.; Wiczk, W.; Gryczynski, I.; Fishman, M.; Johnson, M. *Macromolecules* **1993**, *26*, 349.
(21) Guillet, J. E.; Rendall, W. A. *Macromolecules* **1986**, *19*, 224.
(22) Hu, Y.; Kramer, M. C.; Boudreaux, C. J.; McCormick, C. L. *Macromolecules* **1995**, *28*, 7100.
(23) Smith, G. L.; McCormick, C. L. *ACS Polym. Prepr.* **1998**, *39* (1), 310.
(24) Smith, G. L.; McCormick, C. L. *Macromolecules* **2001**, *34*, 918.
(25) Evans, H. C. *J. Chem. Soc.* **1956**, 579.
(26) Annable, T.; Buscall, R.; Ettelaie, R.; Shepherd, P.; Whittlestone, D. *J. Rheol.* **1993**, *37*, 695.
(27) Sadeghy, K.; James, D. F. *J. Non-Newtonian Fluid Mech.* **2000**, *90*, 127.
(28) Lauten, R. A.; Nystrom, B. *Macromol. Chem. Phys.* **2000**, *201*, 667.
(29) Green, M. S.; Tobolsky, A. V. *J. Chem. Phys.* **1940**, *14*, 80.
(30) Hu, Y.; Smith, G. L.; Richardson, M. F.; McCormick, C. L. *Macromolecules* **1997**, *30*, 3526.
(31) Petit-Agnely, F.; Iliopoulos, I. *J. Phys. Chem. B* **1999**, *103*, 4803.
(32) Guillaumont, L.; Bokias, G.; Iliopoulos, I. *Macromol. Chem. Phys.* **2000**, *201*, 251.

MA001554P